

Ballistic transport in graphene beyond linear response

B. Rosenstein,^{1,*} M. Lewkowicz,² H. C. Kao,³ and Y. Korniyenko¹

¹*Electrophysics Department, National Chiao Tung University, Hsinchu, 30050 Taiwan, Republic of China*

²*Applied Physics Department, Ariel University Center of Samaria, Ariel 40700, Israel*

³*Physics Department, National Taiwan Normal University, Taipei, 11650 Taiwan, Republic of China*

(Received 24 November 2009; published 29 January 2010)

The process of coherent creation of particle-hole excitations by an electric field in graphene is quantitatively described beyond linear response. We calculate the evolution of current density, number of pairs and energy in ballistic regime for electric field E using the tight-binding model. While for ballistic flight times smaller than $t_{nl} \propto E^{-1/2}$ current is linear in E and independent of time, for larger ballistic times the current increases after t_{nl} as $J \propto E^{3/2}t$ and finally at yet larger times ($t > t_B \propto E^{-1}$) Bloch oscillations set in. It is shown that the number of pairs follows the 2D generalization of the Schwinger's creation rate $n \propto E^{3/2}$ only on certain time segments with a prefactor different from that obtained using the asymptotic formula.

DOI: [10.1103/PhysRevB.81.041416](https://doi.org/10.1103/PhysRevB.81.041416)

PACS number(s): 73.61.-r, 11.10.Kk, 73.20.Mf, 73.23.Ad

I. INTRODUCTION

It became increasingly evident that electronic mobility in graphene is extremely large exceeding that in best semiconductor two-dimensional (2D) samples.¹ Since the system is so clean the transport becomes ballistic, especially in suspended graphene samples^{2,3} so that interactions of electrons with phonons, riplons, disorder and among themselves can be neglected. Therefore there is a chance to observe various theoretically predicted exotic phenomena like nonlinear response and Bloch oscillations.⁴

Generally ballistic transport occurs due to two distinct phenomena. If a mobile charge carrier is available (as in an electron gas in a metal), electric field accelerates it, so that current increases linearly in time. In addition, an electric field can create new charge carriers (the process typically suppressed by energy gaps). A peculiarity of the ballistic transport in graphene with the Fermi level pinned right on the two Dirac points⁵ (which happens naturally in suspended graphene samples²) is that there are no charge carriers present at all. The Fermi surface therefore shrinks to just two points. The carriers are created solely by an applied electric field like in the Zener tunneling effect in semiconductors,⁴ but energy gap vanishes due to "ultrarelativistic" dispersion relation, $\varepsilon = v_g |\mathbf{k}|$, where $v_g \sim 10^6$ m/s is the graphene velocity.

The electron-hole pairs are created fast enough to make the current linear in electric field and constant in time, so that it looks like a Drude type linear response due to disorder rather than the ballistic acceleration $J \propto t$ of an electron gas with finite carrier density. The illusion of the "Ohmic" behavior however cannot continue indefinitely in the absence of scatterers, and should eventually cross over to some sort of "acceleration" or even Bloch oscillations at large times. The behavior is expected to become nonlinear as function of electric field as indicated by the nonlinearity of the pair-creation rate. It was shown long time ago,⁶ in the context of particle physics, that the pair-creation rate at asymptotically large times is proportional to $E^{3/2}$.

Ambiguities in the application of the standard Kubo approach for the ultrarelativistic spectrum⁷ led us to propose a dynamic approach to the tight-binding model of graphene.⁸ Within leading order in E (linear response) we found that the

dc conductivity is $\sigma_2 = \frac{\pi e^2}{2h}$ rather than the often cited value $\frac{4e^2}{\pi h}$ obtained from the Kubo formula.⁹ In this note we solve the tight-binding model for arbitrary constant electric field. The evolution of current density demonstrates that the cross-over from the "Ohmic" regime to the nonlinear one occurs at the experimentally achievable time scale $t_{nl} \propto E^{-1/2}$. Bloch oscillations are shown to set in on scale $t_B \propto E^{-1}$ much longer than t_{nl} for experimentally accessible dc electric fields. We discuss the relevance of the 2D generalization of the Schwinger's creation rate formula¹⁰ to physics of graphene.

II. TIGHT-BINDING MODEL AND ITS EXACT SOLUTION

Electrons in graphene are described sufficiently well for our purposes by the 2D tight-binding model of nearest-neighbor interactions on a honeycomb lattice.⁵ The Hamiltonian in momentum space is

$$\hat{H} = \sum_{\mathbf{k}} (c_{\mathbf{k}}^{1\dagger} \quad c_{\mathbf{k}}^{2\dagger}) H_{\mathbf{p}} \begin{pmatrix} c_{\mathbf{k}}^1 \\ c_{\mathbf{k}}^2 \end{pmatrix}, \quad H_{\mathbf{p}} = \begin{pmatrix} 0 & h_{\mathbf{p}} \\ h_{\mathbf{p}}^* & 0 \end{pmatrix}, \quad (1)$$

where

$$h_{\mathbf{p}} = -\gamma \left[\exp\left(i \frac{ap_y}{\sqrt{3}}\right) + b \exp\left(-i \frac{ap_y}{2\sqrt{3}}\right) \right] \quad (2)$$

with $\gamma = 2.7$ eV being the hopping energy and sum is over the Brillouin zone. Nearest neighbors are separated by distance $a = 3 \text{ \AA}$ and $b = 2 \cos(ak_x/2)$ and pseudospin index denotes two triangular sublattices. We consider the system in a constant and homogeneous electric field E along the y direction switched on at $t=0$. It is described by the minimal substitution $\mathbf{p} = \hbar \mathbf{k} + \frac{e}{c} \mathbf{A}$ with vector potential $\mathbf{A} = (0, -cEt)$ for $t > 0$. Since the crucial physical effect of the field is a coherent creation of electron-hole pairs, mostly near the two Dirac points, a convenient formalism to describe the pair creation is the "first quantized" formulation described in detail in Refs. 8 and 11. To consider the ballistic transport at zero temperature, $T=0$ dynamically, one starts at time $t=0$ from the zero-field state in which all the negative-energy one-particle states, $-|h_{\mathbf{k}}| \equiv -\varepsilon_{\mathbf{k}}$, are occupied. The second

quantized state evolving from it is uniquely characterized by the first quantized amplitude,

$$\psi_{\mathbf{k}}(t) = \begin{pmatrix} \psi_{\mathbf{k}}^1(t) \\ \psi_{\mathbf{k}}^2(t) \end{pmatrix}, \quad (3)$$

which is a ‘‘spinor’’ in the sublattice space. It obeys the matrix Schroedinger equation

$$i\hbar\partial_t\psi_{\mathbf{k}} = H_{\mathbf{p}}\psi_{\mathbf{k}}. \quad (4)$$

It is a peculiar property of tight-binding matrix Eq. (1) that solution for arbitrary k_y can be reduced to that for $k_y=0$ and has the Fourier series

$$\psi_{\mathbf{k}}^1(t) = \sum_{s=\pm 1} A^s \sum_{m=-\infty}^{\infty} p_m^s \exp(-i\omega_m^s \bar{t})$$

$$\psi_{\mathbf{k}}^2(t) = - \sum_{s=\pm 1} A^s \sum_{m=-\infty}^{\infty} \frac{p_m^s + bp_{m-1}^s}{\omega_m^s} \exp(i\omega_m^s \bar{t}), \quad (5)$$

where $\bar{t} = t - t_\gamma a k_y / \mathcal{E}$ and $\omega_m^s = \omega^s + 3\Omega m$ for frequency $\Omega = \mathcal{E} / (2\sqrt{3}t_\gamma)$; $\mathcal{E} = E/E_0$. The relevant microscopic time scale is $t_\gamma = \hbar / \gamma$ and field $E_0 = \gamma / (ea)$. Recursion relations for the Fourier amplitudes p_m ,

$$p_m = [(\omega_m^2 - 8\Omega\omega_m + 15\Omega^2 - 1)/b - b(\omega_m - 5\Omega)]p_{m-1} - \frac{\omega_m - 2\Omega}{\omega_m - 5\Omega} p_{m-2}, \quad (6)$$

has two solutions p^s , $s = \pm 1$ with two Floquet frequencies¹² ω^s . The recursion is easily solved numerically and has the following convergent expansion in b in the whole relevant range, $0 < b \leq 2$,

$$\omega^s = \omega_0^s + \frac{b^2}{\omega_0^{s2} - \Omega^2} \left[\frac{\omega_0^s - 2\Omega}{6\Omega(2\omega_0^s + \Omega)} + \frac{\omega_0^s}{2} - \Omega \right] - \frac{b^2(\omega_0^s - 5\Omega)}{6\Omega(\omega_0^s - \Omega)(\omega_0^s - 2\Omega)(2\omega_0^s - 5\Omega)} + O(b^4), \quad (7)$$

with $\omega_0^s = s\Omega + \sqrt{t_\gamma^{-2} + \Omega^2}$. It turns out that the two Floquet frequencies obey the relation obeying $\omega^+ = 2\Omega - \omega^-$, again peculiar to graphene, as can be checked by both the perturbation theory, Eq. (7), and numerical results. For experimentally accessible cases $\Omega \ll t_\gamma^{-1}$ and the frequencies are just $\pm t_\gamma^{-1}$. Coefficients A^s are fixed by initial conditions

$$\psi_{\mathbf{k}}(t=0) = u_{\mathbf{k}} = \begin{pmatrix} 1 \\ -h_{\mathbf{k}}^*/\varepsilon_{\mathbf{k}} \end{pmatrix}. \quad (8)$$

This solution is used to calculate evolution of current density, energy and the number of electron-hole pairs.

III. TIME SCALE FOR OBSERVATION OF THE BLOCH OSCILLATIONS IN GRAPHENE

Evolution of the current density during the ballistic ‘‘flight time’’ t_{bal} is the integral over Brillouin zone (multiplied by factor 2 due to spin),⁸

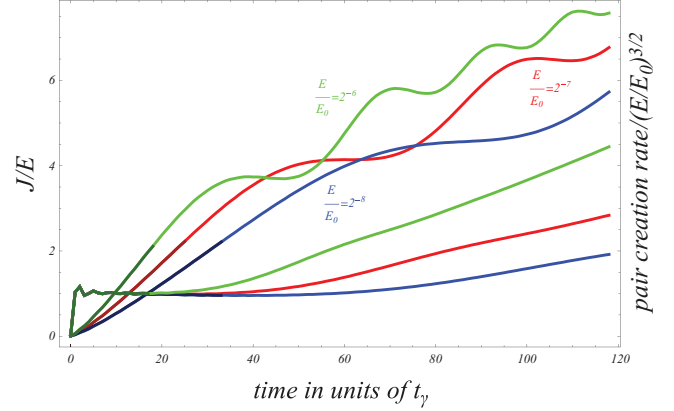


FIG. 1. (Color) The time evolution of the current density (three bottom curves) and the scaled pair creation rate (three top curves) at relatively short times for various fields. The shaded parts indicate the linear response periods.

$$J_y(t) = -2e \sum_{\mathbf{k}} \psi_{\mathbf{k}}^\dagger(t) \frac{\partial H_{\mathbf{p}}}{\partial p_y} \psi_{\mathbf{k}}(t). \quad (9)$$

The current density divided by electric field, $\sigma(t) \equiv J_y(t)/E$, is shown in Figs. 1 and 2 for various values of the dimensionless electric field \mathcal{E} in the range $2^{-8} - 2^{-5}$.

Fig. 1 in which evolution is shown up to ballistic time of $120t_\gamma$ demonstrates that after an initial fast increase on the microscopic time scale t_γ (shown in more detail, using linear response, in Ref. 8), $\sigma(t)$ approaches the universal value σ_2 and settles there. Beyond linear response one does not expect the current density to hold up to this value indefinitely. In a ballistic system the energy initially increases, as follows from the Joule law. The total energy of electrons can be written in the first quantized formalism as

$$U_{tot}(t) = 2 \sum_{\mathbf{k}} \psi_{\mathbf{k}}^\dagger(t) H_{\mathbf{p}} \psi_{\mathbf{k}}(t) \equiv 2 \langle \psi(t) | H | \psi(t) \rangle. \quad (10)$$

It can be shown using Eq. (4) that the power

$$P(t) = \frac{d}{dt} U_{tot} = 2 \langle \psi | \frac{d}{dt} H | \psi \rangle = -2eE \langle \psi | \frac{\partial H_{\mathbf{p}}}{\partial p_y} | \psi \rangle = EJ_y(t), \quad (11)$$

is indeed proportional to current density. Since in the tight-binding model electron’s energy cannot exceed the upper

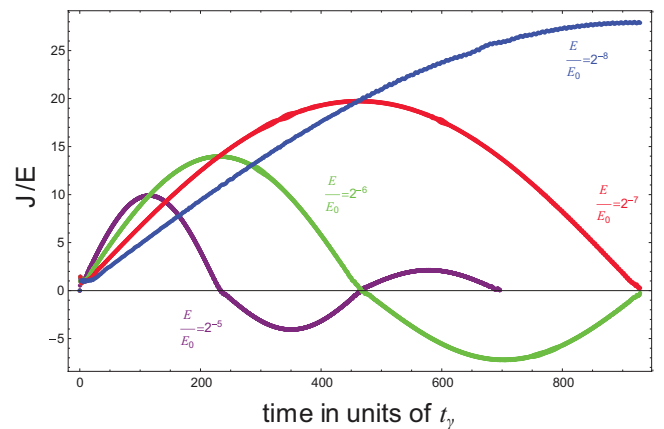


FIG. 2. (Color) The time evolution of the current density is shown for various fields up to $1000t_\gamma$.

band-edge energy 3γ , hence at some time scale t_B the energy increase is reversed. The physics which takes over is that of the Bloch oscillations and is similar to that in ordinary materials, namely, electrons' energies are elevated by the electric field⁴ due to the quasimomentum shift. This feature is not related to the unique "relativistic" feature of the graphene spectrum.

The current, shown in Fig. 2 for ballistic times up to $1000t_\gamma$, indeed exhibits Bloch oscillations. It turns out that the current vanishes at points given *exactly* at multiples of $t_B/2$ with

$$t_B = \frac{8\pi}{\sqrt{3}} \frac{\hbar}{eEa} = \frac{8\pi t_\gamma}{\sqrt{3} \mathcal{E}} \quad (12)$$

being the period of the Bloch oscillations. The Bloch time is approximately the time required for the electric field to shift the momentum across the Brillouin zone $\Delta p_y = eEt_B \sim \hbar/a$. These times are very long for experimentally achieved fields, much longer than the ballistic flight time. One observes in Fig. 2 another peculiar feature that (apart from the "relativistic" initial constant segment) time dependence of $\sigma(t)$ is similar for different electric fields. Indeed, if one plots J/\sqrt{E} versus tE , all the curves nearly coincide. Moreover

$$J(t) = \sqrt{3} \sigma_2 E_0^{1/2} E^{1/2} \sin\left(\frac{2\pi t}{t_B}\right) \quad (13)$$

is an excellent fit.

For a sample of submicron dimensions, $L=0.5 \mu\text{m}$, $W=1.5 \mu\text{m}$, the ballistic time can be estimated as $t_{bal}=L/v_g \approx 2.3 \cdot 10^3 t_\gamma$ with $v_g = \frac{\sqrt{3}}{2} \frac{\gamma a}{\hbar}$. For large currents (I_{\max} in the mA region) the electric field is $E_{\max} = \frac{I_{\max}}{W\sigma_2} = 10^7 \text{ V/m}$ corresponding to $\mathcal{E}=10^{-3}$ (the voltage would be quite large $V_{\max}=5 \text{ V}$). The first maximum of the Bloch oscillation will be seen at flight time of $t_B/4=3.6 \cdot 10^3 t_\gamma$, which is of the same order as t_{bal} . For a dc current typical to transport measurements $I=50 \mu\text{A}$, the electric field is just $E=5 \times 10^5 \text{ V/m}$ corresponding $\mathcal{E}=5 \times 10^{-5}$, $t_B/4=7.2 \times 10^4 t_\gamma \gg t_{bal}$ and is therefore at this time out of reach. (Yet Bloch oscillations have been experimentally observed for ac fields.¹³)

IV. CROSSOVER FROM LINEAR TO NONLINEAR REGIMES

In Fig. 1 one clearly observes a remarkable feature: there is a much smaller crossover time t_{nl} , after which the conductivity rises linearly with time above the constant "universal" value σ_2 ,

$$J(t) = \sigma_2 \left(\frac{\sqrt{3}}{2} E\right)^{3/2} \left(\frac{e v_g}{\hbar}\right)^{1/2} t. \quad (14)$$

The onset of the nonlinear behavior can hence be defined at

$$t_{nl} = \frac{2^{3/2}}{3^{3/4}} \sqrt{\frac{\hbar}{e E v_g}} \approx \frac{1.3}{\sqrt{\mathcal{E}}} t_\gamma. \quad (15)$$

It becomes the same as the ballistic time $t_{bal}=2.3 \times 10^3 t_\gamma$ mentioned above, for relatively weak fields $E=10^4 \text{ V/m}$

corresponding to $\mathcal{E}=10^{-6}$. Therefore some of the transport measurements performed might be influenced by the physics beyond linear response.

A qualitative picture of this resistivity without dissipation is as follows. The electric field creates electron-hole excitations mostly in the vicinity of the Dirac points in which electrons behave as massless relativistic fermions with the graphene velocity v_g playing a role of velocity of light. For such particles the absolute value of the velocity is v_g and cannot be altered by the electric field and is not related to the wave vector \mathbf{k} . On the other hand, the orientation of the velocity is influenced by the applied field. The electric current is $e\mathbf{v}$, thus depending on orientation, so that its projection on the field direction y is increased by the field. The energy of the system (calculated in a way similar to the current) is increasing continuously if no channel for dissipation is included. Therefore the "Ohmic" conductivity originates in creation of pairs near the Dirac points with an additional contribution due to the alignment of the particles' motion with the field's direction. At times of order t_B his process exhausts itself due to the following processes. Electrons gain momentum from the electric field and leave eventually the neighborhoods of the Dirac points. They are no longer ultrarelativistic and are described by (positive or negative) effective mass⁴ and the more customary physics takes over.

The crossover to the nonlinear regime can be detected from within the perturbation theory in electric field. Indeed we found that the E^2 correction to conductivity is

$$J(t)/E = \sigma_2 \left[1 + \frac{3}{64} \mathcal{E}^2 \frac{t^4}{t_\gamma^4} + O(\mathcal{E}^4) \right]. \quad (16)$$

The correction therefore becomes as large as the leading order for $t=2.1 t_\gamma / \mathcal{E}^{1/2} \approx t_{nl}$. To gain more insight into the nature of the crossover to nonlinear response we calculated also evolution of the energy and number of electron-hole pairs during the ballistic flight.

V. SCHWINGER'S PAIR-CREATION FORMULA AND GRAPHENE

The states in the conduction band for each momentum \mathbf{k} in the Brillouin zone are described by a pseudospinor,

$$v_{\mathbf{k}} = \begin{pmatrix} 1 \\ h_{\mathbf{k}}^* / \varepsilon_{\mathbf{k}} \end{pmatrix} \quad (17)$$

orthogonal to $u_{\mathbf{k}}$ defined in Eq. (8). The amplitude of lifting of an electron into the conduction band is $A_{\mathbf{k}} = \langle \psi(t) | v_{\mathbf{k}} \rangle$ and consequently the density of pairs (factor 2 for spin) reads as

$$N_p(t) = 2 \sum_{\mathbf{k}} |A_{\mathbf{k}}|^2 = 2 \sum_{\mathbf{k}} \left| \psi_1^* + \frac{h_{\mathbf{k}}^*}{\varepsilon_{\mathbf{k}}} \psi_2^* \right|^2, \quad (18)$$

and the rate $\frac{d}{dt} N_p$ is shown in Fig. 1 as function of time. Its time dependence exhibits several time scales. At times smaller than t_{nl} expansion in electric field is applicable and the leading-order result is

$$\frac{d}{dt}N_p = -2 \left(\frac{eE}{\hbar} \right)^2 t \sum_{\mathbf{k}} \left[\frac{\hbar \partial_{p_y} h^* - cc}{\varepsilon^2} \sin \left(\frac{2\varepsilon t}{\hbar} \right) \right]^2. \quad (19)$$

This is analogous to the “linear response” for the current. Immediately after the switching on the electric field (times of order t_γ) the pair-creation rate per unit area behaves as t^3 . For $t_\gamma < t < t_{nl}$ the pair-creation rate per unit area rises linearly (with logarithmic corrections),

$$\frac{d}{dt}N_p \approx \frac{2}{\pi} \left(\frac{eE}{\hbar} \right)^2 t \log \left(\frac{t}{t_\gamma} \right), \quad (20)$$

and is dominated by the neighborhood of the Dirac points.

However it is clear from Fig. 1 that the expansion breaks down at t_{nl} , when the rate stabilizes approximately at

$$\frac{d}{dt}N_p = 3.7 v_g^{-1/2} \left(\frac{eE}{\hbar} \right)^{3/2}.$$

and scales as the power $E^{3/2}$. The rate continues to rise in a series of small jumps till Bloch oscillations set in. At that stage (actually at about $t_B/4$) number of electrons elevated into the conduction band becomes of order one, consistent with Eq. (12). Then it oscillates. The power $E^{3/2}$ is, up to a constant, the same as the rate of the vacuum breakdown due to the pair production calculated beyond perturbation theory by Schwinger in the context of particle physics (when generalized to the 2+1 dimensions and zero fermion mass^{6,10}). This is not surprising since the power $E^{3/2}$ is dictated by dimensionality assuming ultrarelativistic approximation is valid. However the physical meaning is somewhat different. We have used here a definition of the pairs number with respect to Fermi level of the system before the electric field is switched on (equivalently when an electrons are injected into a graphene sheet from a lead). This is different not only from the Schwinger’s path-integral definition in which the Fermi level is “updated” along the work of electric field and from the definition proposed recently¹⁰ in connection with graphene. The asymptotics at very large times is not relevant for experimentally achievable ballistic times, so that the predicted relatively short plateau segments are more important.

VI. SUMMARY

Ballistic transport in single graphene sheet near Dirac point was investigated using the dynamic approach beyond

linear-response theory. We found that, while the observation of the Bloch oscillations is difficult, there exists a time scale t_{nl} , see Eq. (15), of transition to a nonlinear regime which is within reach of current experimental techniques. The physics of the ballistic transport in graphene can be described as a succession of four time segments with different character:

(i) at microscopic ballistic times $t \sim t_\gamma$ the current reacts fast to electric field and depends on microscopic details;

(ii) the current density at zero temperature stays constant $\sigma_2 E$ for ballistic times $t_\gamma < t < t_{nl}$ and physics is partially universal in the following sense. There are generally two contributions to the current. While one contribution is dominated by Dirac points, the other is related to the band structure. However the second contribution vanishes due to symmetry properties of the Brillouin zone, see ref. 8.

(iii) For $t_{nl} < t < t_B$ the current density during the flight would rise above this value. It is dominated solely by the close vicinity of each of the two Dirac points. Perhaps the increase of conductivity might be at least partly responsible for the “missing π ” problem,^{5,14} namely, that experimentally measured minimal conductivity is higher than σ_2 even in suspended samples.²

(iv) Finally at $t \sim t_B$ Bloch oscillations set in. The physics is again dominated again by the band structure, is “nonrelativistic” and is not directly related to the Dirac points.

It should be noted that in addition to limitations of the tight-binding model used which ignores impurities, interactions, deviation of the chemical potential from the Dirac point and temperature beyond linear response such “relativistic” effects like the pair annihilation neglected. For very large electric fields the effects of radiation of energy into space (radiative friction) might in principle be observable and should be investigated. On the other hand influence of temperature and nonzero chemical potential in nonlinear regime are expected to be similar to those in linear response studied in Ref. 8.

ACKNOWLEDGMENTS

We are grateful to S. Gurvitz, E. Andrei, A. Morpurgo, J. Goltzer, and W. B. Jian for discussions. Work of B.R., Y.K., and H.K. was supported by NSC of R.O.C. Grant No. 98-2112-M-009-014-MY3 and 98-2112-M-003-002-MY3, respectively, and MOE ATU program. B.R. acknowledges the hospitality of the Applied Physics Department of AUCS; M.L. acknowledges the hospitality and support at Physics Department of NCTU.

*vortexbar@yahoo.com

¹S. V. Morozov *et al.*, Phys. Rev. Lett. **100**, 016602 (2008).

²X. Du *et al.*, Nat. Nanotechnol. **3**, 491 (2008).

³K. I. Bolotin *et al.*, Solid State Commun. **146**, 351 (2008).

⁴J. H. Davis, *The Physics of Low Dimensional Semiconductors* (Cambridge University Press, New York, 1998).

⁵A. H. Castro Neto *et al.*, Rev. Mod. Phys. **81**, 109 (2009).

⁶J. Schwinger, Phys. Rev. **82**, 664 (1951).

⁷K. Ziegler, Phys. Rev. B **75**, 233407 (2007).

⁸M. Lewkowicz and B. Rosenstein, Phys. Rev. Lett. **102**, 106802 (2009).

⁹E. Fradkin, Phys. Rev. B **33**, 3257 (1986); P. A. Lee, Phys. Rev.

Lett. **71**, 1887 (1993); V. P. Gusynin and S. G. Sharapov, Phys. Rev. B **73**, 245411 (2006).

¹⁰A. Casher *et al.*, Phys. Rev. D **20**, 179 (1979); D. Allor *et al.*, *ibid.* **78**, 096009 (2008).

¹¹E. S. Fradkin *et al.*, *Quantum Electrodynamics with Unstable Vacuum* (Springer-Verlag, Berlin, 1991).

¹²C. Chicone, *Ordinary Differential Equations with Applications* (Springer-Verlag, New York, 1999).

¹³D. Dragoman and M. Dragoman, Appl. Phys. Lett. **93**, 103105 (2008).

¹⁴K. S. Novoselov *et al.*, Nature (London) **438**, 197 (2005); Y. Zhang *et al.*, *ibid.* **438**, 201 (2005).